JOURNAL OF MATERIALS SCIENCE 29 (1994) 3601–3606

Silica fracture

Part I *A ring contraction model*

J. K. WEST, L. L. HENCH
Advanced Materials Research Center, Department of Materials Science and Engineering, University of Florida, Gainesville, FL 32610, USA

A quantitative ring contraction model for the fracture of amorphous silica is described based upon AM-1 semiempirical molecular orbital calculations of strained three- and four-fold silica rings and a five-fold ring-chain structure. The fracture barrier for five-fold ring-chain structures is 103 kcal mol^{-1}. The barrier for fracture of a three-fold ring is 96 kcal mol^{-1}. Fracture by contraction of four-fold rings has a lower energy barrier of 77 kcal mol^{-1} due to formation of pentacoordinate silicon transition states which produce trisiloxane rings and a broken siloxane bond. Thus, the ring contraction model predicts that a crack will follow a path which depends on the distribution of four-fold (or larger) rings in vacuum or fast fracture.

1. Introduction

It has been recognized since the time of Inglis [1] and Griffith [2] that fracture occurs on an atomistic level when the bonds between the atoms are strained past the breaking point. When a tensile stress at the tip of a crack exceeds a critical value, crack growth will occur [3]. This fundamental concept underlying fracture is typically modelled as a continuous stress–displacement curve, approximated as a sine curve. However, because of structural constraints and the finite size of molecular bonds, a crack tip must advance in increments, with the size of the step dictated by the localized structure containing the crack tip. A continuum of strain applied to a material must be translated mechanistically into quantitized steps of bonds breaking.

The difficulty in developing a quantitative atomistic theory of fracture is modelling the localized strain of bonds to the point of breaking within an assembly of atoms large enough to represent the constraints and structural features of the neighbouring strained, but unbroken, bonds. Recently, Simmons *et al.* [4] have used molecular dynamics (MD) to model fracture in amorphous SiO_2. They show that at the crack tip, silicon atoms adjust to the local strain by retreating below an "oxygen-rich surface" as Si–O bonds are broken. However, MD models cannot yield the reaction pathways or energy barriers to the fracture event. A quantitative description of metastable, activated transition states involved in bond breaking cannot be achieved in MD simulations or in most of the other fracture-modelling efforts reported [5, 6]. An MD simulation of bond breaking of the same polysiloxane rings discussed here does not yield any transitional states during fracture. The intermediate states are not observed in MD owing to the limitations of the force function approximations. In contrast, the latest generation of semi-empirical molecular orbital theory does not have these force function restrictions.

Our goal was to use the latest generation of semi-empirical molecular orbital theory to model the effects of bond strain on silicate structures containing different numbers of tetrahedra. The effects of ring size on bond breaking have been calculated, thereby representing localized structural constraints. In Part I we describe the reaction pathway for fracture of polysiloxane rings *without* the presence of water. A fracture mechanism of progressive ring contraction is discovered with a quantitized transition state barrier to fracture of 77–79 kcal mol^{-1}. In Part II we describe the reaction pathway for fracture of polysiloxane rings in the presence of water. A much lower energy process of ring opening occurs via hydrolysis, with only a 7 kcal mol^{-1} barrier.

2. AM-1 molecular orbital method

In this study we use AM-1 molecular orbital theory [7, 8] within the parameters of MOPAC 5.0 and 6.1 [9]. Burggraf and co-workers have shown that the modified neglect of the diatomic overlap (MNDO) semi-empirical MO method can be used to model the reactions of silicon-containing molecules [10, 11]. However, there are two situations in which MNDO produces large errors. MNDO overestimates core–core repulsions between atoms when they are separated by approximately van der Waals distances. This means that MNDO cannot reproduce hydrogen-bonds or accurately calculate the heat of formation, H_f, for strained or crowded molecules, such as those involved in bond breaking. The MNDO method also overestimates transition state energies and distorts transition state geometries, again fatal flaws for calculating bond-fracture mechanisms. The Austin Method (AM1) [7, 8], a semi-empirical method, reduces these problems by modifying the core-repulsion function used in MNDO with additional Gaussian terms, and

0022–2461

the calculated structures and heats of formation match quite well with experimental values [7, 8].

In studying fracture it is necessary to be aware of the limitations of the AM1 method. A model of simple Si–O bond breaking will not yield realistic results due to creation of unpaired electrons in the reaction. AM1, and other semi-empirical methods, does not include the wavefunctions for unpaired electrons. This limitation is overcome by using *ab initio* generalized valence bond (GVB) theory. However, the GVB level of theory is difficult to apply to structures large enough to simulate a fracture process [12].

A limitation in the physics of the AM-1 theory is that antibonding wavefunctions are ignored. However, during bond breaking, anti-bonding wavefunctions may be important. Therefore, in order to determine the magnitude of this problem with AM1, Si–O bond fracture was modelled using restricted Hartree Fock (RHF), unrestricted Hartree Fock (UHF) and configuration interaction (CI) methods within the parameters of MOPAC.

The restricted Hartree Fock approximation has one wavefunction for each pair of electrons. Thus, fracture of a bond involving electron pairs will be inaccurately modelled with RHF. The unrestricted Hartree Fock approximation is a higher order theory which includes a wavefunction for each electron in a bond. Consequently, bond breaking in a UHF model will more closely approximate the physics of the configuration. It is a much longer calculation to run the UHF approximation and therefore the computational strategy used in the work was first to identify transition states in the reaction path of bond breaking using RHF. The critical geometries achieved with the RHF calculation were then submitted for UHF optimization and energy calculations. The complexity of the transition state structures would have been nearly impossible to identify directly by the UHF model. The configuration

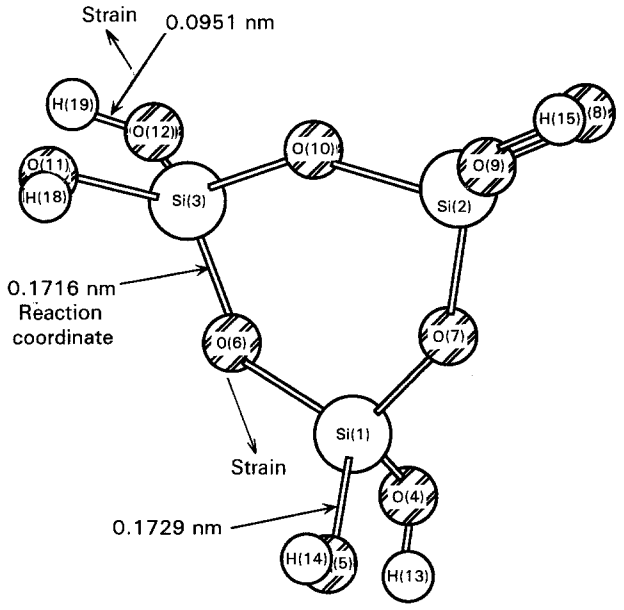

AM1 UHF heat of formation = -727.57 kcal mol^{-1} (Model BB13)

Figure 1 AM1 structure of cyclotrisiloxane (three-fold ring).

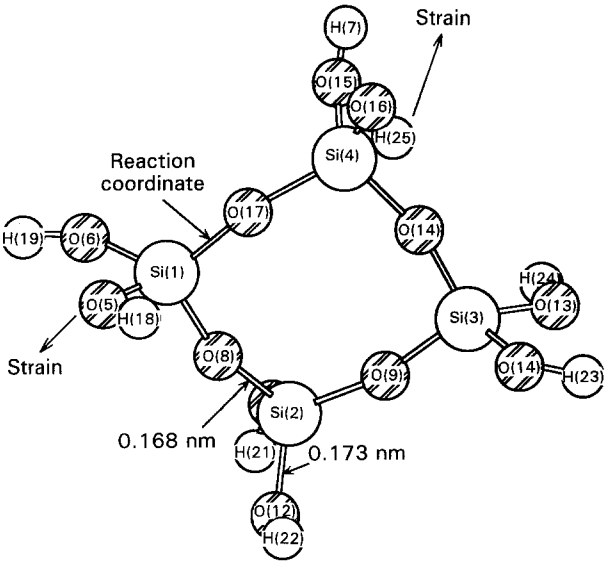

AM1 UHF heat of formation = − 992 kcal mol^{-1}
(Model R4)

Figure 2 AM1 structure of a cyclotetrasiloxane (four-fold) ring.

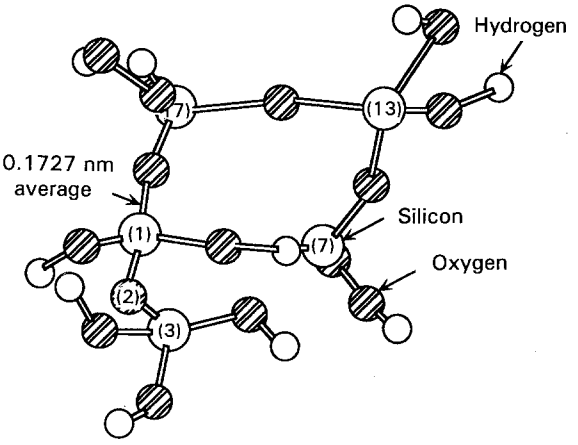

Ring-chain structure
AM1 heat of formation = -1237.8 kcal mol^{-1}
(MOPAC 5.0)

Figure 3 Initial AM1 model of a five-fold silica ring-chain structure.

interaction (CI = 3) model is an extension of the UHF approximation where electrons are excited into higher molecular orbitals during the calculation.

In this study, these three approaches were applied to modelling the water-free fracture of a three-fold silica ring (Raman D_2 cyclotrisiloxane), a four-fold silica ring (cyclotetrasiloxane), and a five-fold silica ring-chain cluster. These optimized structures are shown in Figs 1–3, respectively. Some earlier calculations were done using MOPAC 5.0. The heats of formation obtained for the silica reactions are nearly identical for both MOPAC 5.0 and 6.1. However, important features were recalculated using the newer 6.1 version.

3. Results of bond-fracture models

3.1. Three-fold silica ring water-free fracture

A reaction coordinate calculation was done using MOPAC 6.1 on a cyclotrisiloxane molecule (Fig. 1).

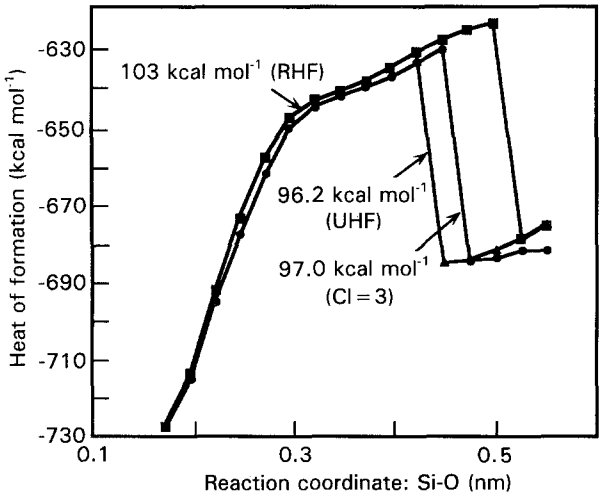

Figure 4 Reaction path for water-free fracture of a cyclotrisiloxane ring. (□) RHF, (+) UHF, (△) CI-3.

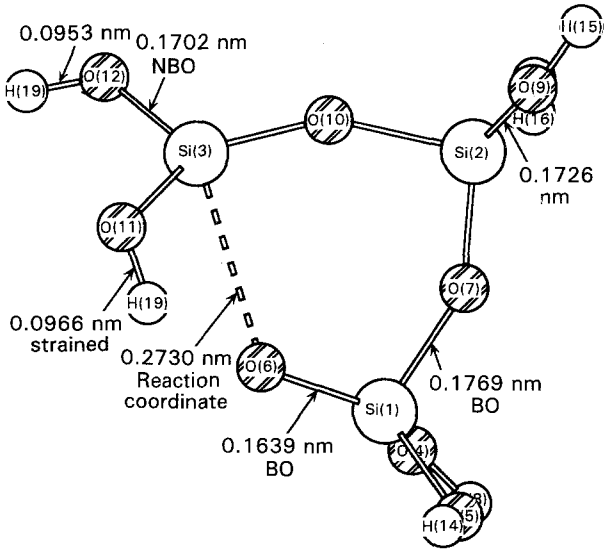

AM1 UHF heat of formation = -657.87 kcal mol^{-1}
(Model BB23-2.730)

Figure 5 Strained Si–O bond distance of 0.2730 nm in the water-free fracture of cyclotrisiloxane.

One of the Si–O bond distances (Si(3)–O(6)) was strained in 0.02 nm increments during the optimized search. No intermediate transition state structures or energy minima were obtained as shown in Fig. 4. Fracture occurred at an energy, ΔE, of 103 kcal mol^{-1} in the RHF calculation. The value of > 100 kcal mol^{-1} is similar to experimental values for fracture of vitreous silica in a vacuum [6].

The calculation was repeated using UHF, with 0.02 nm increments of strain. The UHF calculation followed the RHF within a few tenths of a kcal mol^{-1} until the Si–O bond fractured. Fig. 4 shows that the barrier to fracture for UHF is slightly less at + 96.2 kcal mol^{-1}. Details of the structural evolution is shown in the sequence of Figs 1, 5–7. The final structure is not realistic for bulk materials. We would expect the crack tip to propagate and the bulk would constrain the opened ring from re-closing. The transition state then is the important feature which looks like an open three-fold chain (Fig. 6).

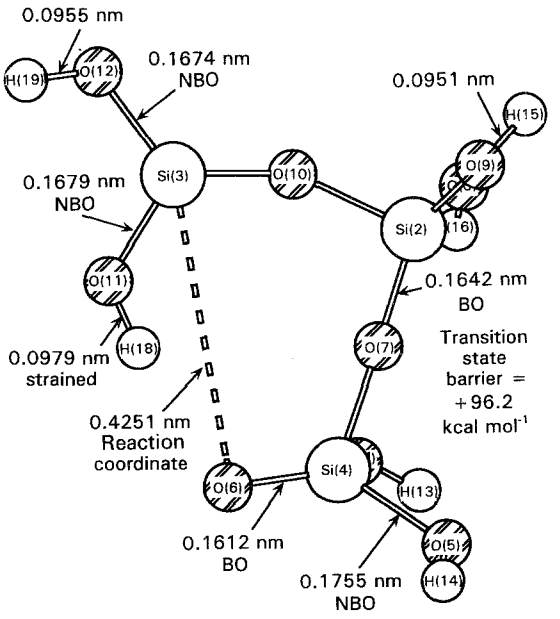

AM1 UHF heat of formation = -631.41 kcal mol^{-1}
(Model BB23-4.251)

Figure 6 Transition state in the water-free fracture of the Si–O bond in cyclotrisiloxane with a barrier of + 96.2 kcal mol^{-1}.

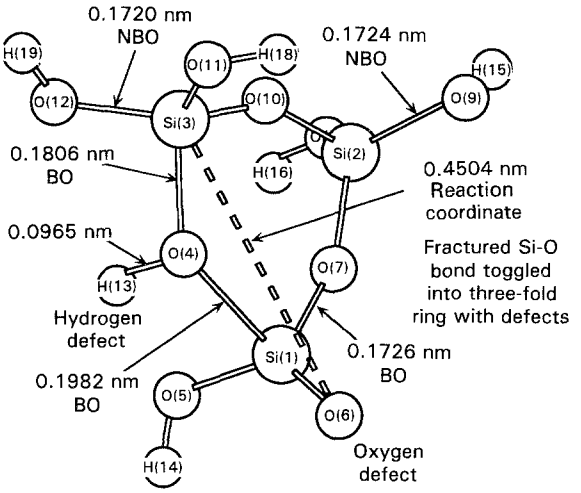

AM1 UHF heat of formation = -685.7 kcal mol^{-1}
(Model BB23-4.504)

Figure 7 Fractured Si–O bond showing the formation of an intermediate cyclotrisiloxane structure with both an oxygen and a hydrogen defect.

The calculation was repeated again with 0.02 nm increments of strain using the CI = 3 method. The results are also shown in Fig. 4. The CI = 3 barrier to fracture is 97.0 kcal mol^{-1}. All three fracture models follow the same general trend until the Si–O bond fractures.

There are small differences in the amount of strain to fracture (0.43–0.50 nm) and the energy to break the Si–O bond (Fig. 4). Results from the UHF and CI methods are within the uncertainty of the AM1 mode

[8]. We, therefore, use the UHF value for generalization throughout the study.

3.2. Four-fold silica ring water-free fracture

The four-fold silica ring, called the D_1 Raman defect [13], used to model Si–O bond fracture, is shown in Fig. 2. The ring was strained to break the Si(1)–O(17)

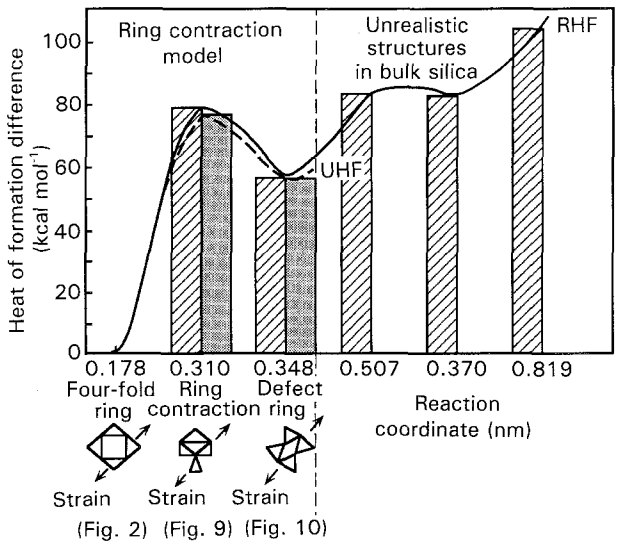

Figure 8 Reaction path for the Si–O bond fracture for a cyclotetrasiloxane (four-fold) ring.

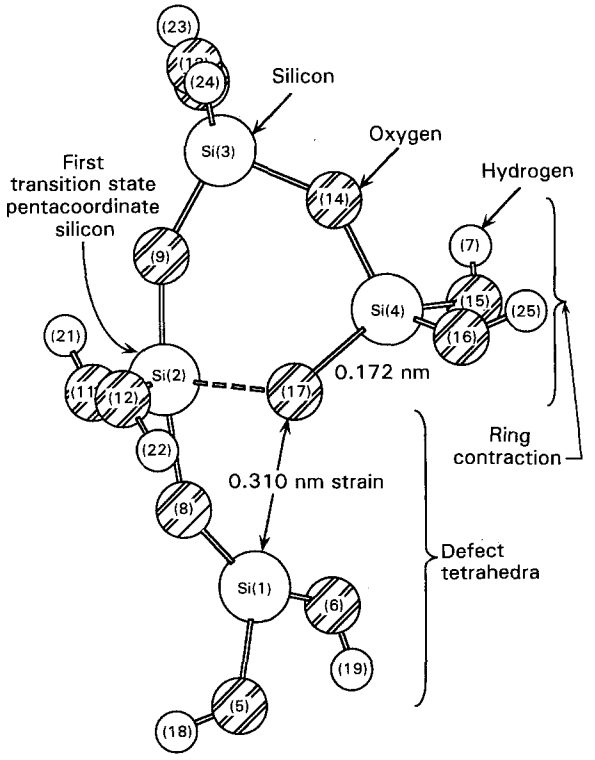

AM1 RHF heat of formation = -923.4 kcal mol^{-1}
(Model BB11)
AM1 UHF heat of formation = -925.9 kcal mol^{-1}
(Model BB36)

Figure 9 First transition state for the Si–O bond fracture without water in a cyclotetrasiloxane (four-fold ring).

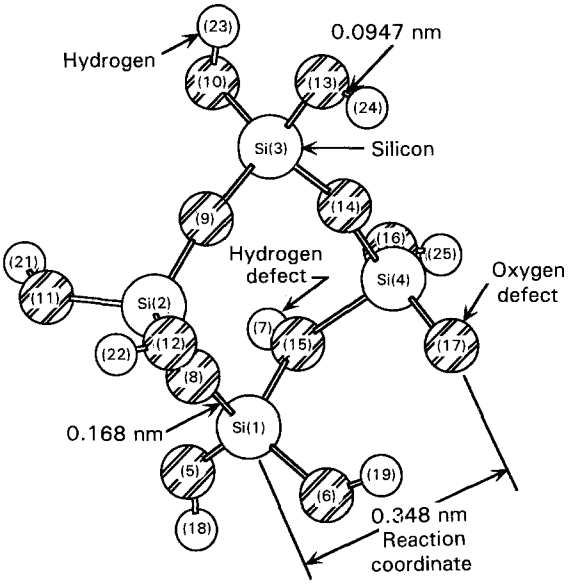

AM1 RHF heat of formation = -946.2 kcal mol^{-1}
(Model BB22)
AM1 UHF heat of formation = -946.2 kcal mol^{-1}
(Model BB27)

Figure 10 The intermediate optimized structure between the two transition states in the Si–O bond fracture of a cyclotetrasiloxane (four-fold) ring without water interaction.

bond without the presence of water. The strain was applied in 0.01 nm increments during an optimized reaction coordinate calculation using AM1 RHF. Two maxima were found, as shown in Fig. 8. The transition state structure associated with the first maximum is shown in Fig. 9. The geometry clearly shows that the four-fold ring has contracted into a three-fold ring and a defect tetrahedron. The three-fold ring and the defect tetrahedron share a pentacoordinate silicon (Si(2)). The intermediate state between the two maxima is shown in Fig. 10. Note that this metastable intermediate state structure is a four-fold ring with a hydrogen defect and an oxygen defect. It is a logical energy minimum in Fig. 8. This four-fold defect ring is probably not realistic in the fracture of bulk silica due to matrix constraints which would prevent formation of the Si(1)–O(15)–Si(4) siloxane bond. The important feature once again is the transition state (Fig. 9). This metastable intermediate represents the ring contraction as the crack tip encounters a cyclotetrasiloxane structure in a-SiO_2.

The energetics of water-free fracture of the four-fold silica ring are summarized in Fig. 8. Both the RHF and UHF models show very similar results. As in cyclotrisiloxane fracture (Fig. 4), the RHF model slightly overestimates the heat of formation. The UHF four-member ring fracture barrier is 77 kcal mol^{-1} leaving a three-member ring behind as the crack tip moves to the next lowest energy process. If the crack tip does not encounter another four-membered ring, it either must break the defect tetrahedron away from the contracted ring, or open the contracted three-membered ring. In the next section we model the removal of the tetrahedron from a ring structure.

3.3. Five-fold ring-chain structure water-free fracture

A five-fold ring-chain structure was chosen to represent Si–O bond breaking in the presence of a neighbouring silica structural unit that remains intact. This provides a closer representation of the local environment of a crack tip if no rings are within the radius of the strain field. Fig. 3 shows the ring-chain structure which consists of a four-fold ring, equivalent to Fig. 2, with a silicic acid molecule bonded to the ring by means of the Si(1)–O(2) siloxane bond. This is the bond to be broken in the calculations.

An initial reaction coordinate optimized search calculation was done on the Si(1)–O(2) bond fracture without water using MOPAC 5.0 and RHF. The bond was strained in 0.01 nm increments. Fig. 11 shows the structure with a fractured Si(1)–O(2) bond for a strain of 0.290 nm. The four oxygens nearest to Si(1) have been strained into a planar structure as the Si(1)–O(2) bond was elongated. The oxygens have toggled towards the fractured bond, thus effectively shielding the silicon atom, Si(1), from the fracture "surface". The energy path of the bond fracture is shown in Fig. 12. The toggling, or planar strain, process results in an inflection in the fracture path energetics for the RHF model. The energy barrier for fracture was 84 kcal mol^{-1}. This value is too low and is due to the calculation being done with the RHF approximation where only one wavefunction is used to describe each pair of electrons as discussed earlier.

The calculation was repeated using both UHF and CI = 3 in AM1. These results are similar to the RHF calculation, but without the inflection (Fig. 12). The Si–O bond is strained significantly to 0.33–0.38 nm before fracture, as shown in Fig. 12. The UHF

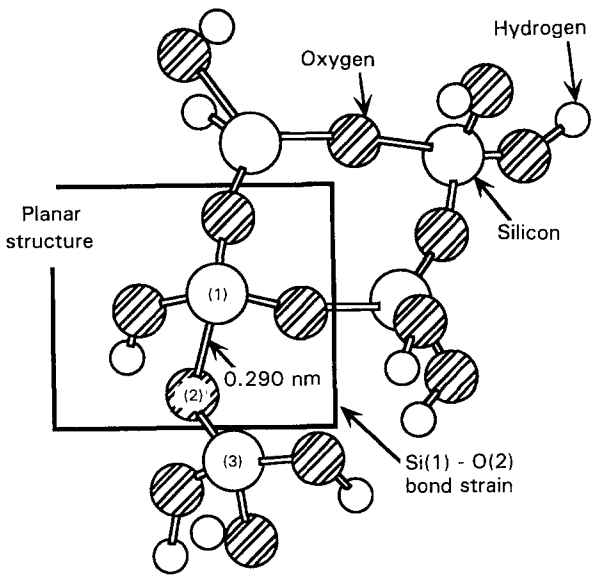

Figure 11 The transition state for Si–O bond fracture of a five-fold ring-chain structure that creates a planar defect.

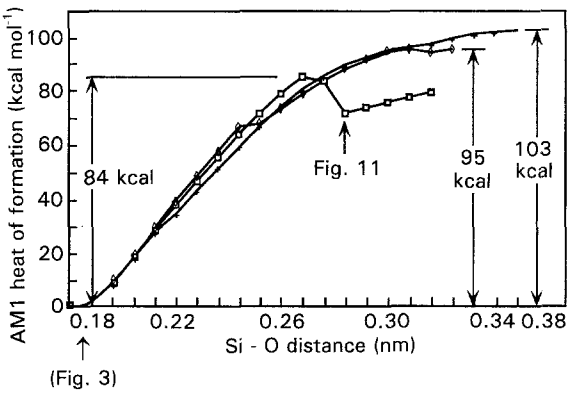

Figure 12 The reaction paths for water-free Si–O bond fracture in a five-fold ring-chain structure with three different levels of MO theory: (□) RHF, (+) UHF, (◇) CI = 3.

barrier for the ring-chain water-free fracture is 103 kcal mol^{-1}. The CI = 3 barrier is 95 kcal mol^{-1}.

The values for ring-chain water-free fracture compare well with the UHF value of 96 kcal mol^{-1} and CI = 3 value of 97 kcal mol^{-1} for cyclotrisiloxane water-free fracture (Fig. 4). We expect the ring strain in the cyclotrisiloxane structure [13] to lower the fracture barrier somewhat (7 kcal mol^{-1}), as was found using UHF theory.

4. Discussion

The important finding from these calculations is the development of intermediate, transition state structures when a four-membered silicate ring is strained. The four-fold ring contracts into a three-fold ring and a defect tetrahedron which share a pentacoordinate silicon. The energy required to form the transition state structure is 20 kcal mol^{-1} *less* than required to break a Si–O bond in a three-membered ring or to pull a tetrahedron off a four-membered ring, as summarized in Fig. 13. Thus, water-free fracture of a four-fold (D_1) ring appears to be most energetically favourable by about 20 kcal mol^{-1}.

The structural reason for the lower energy of bond fracture is that the MO model used herein strains "both halves" of the four-fold ring. Consequently, the four-fold ring is able to adjust siloxane bond angles to accommodate the increase in bond distances. The angular changes create a local MO environment whereby the transition state structures with pentacoordinate silicon have a lower energy configuration. The strain essentially forces localized sp^3d hybridization of the electrons of the silicon atom at the crack tip, thus storing the strain energy in the form of electronic exitations. As the crack propagates, the electronic exitations will be released as a quantitized spectrum of photons and phonons. Only a bond strain model that is capable of creating such angular adjustments of electronic orbitals will provide a realistic approximation to the phenomena occurring at a crack tip.

The three-fold ring, Raman D_2 defect, is more difficult to break. This is understood by examining the transition states in the fracture of the four-fold, D_1

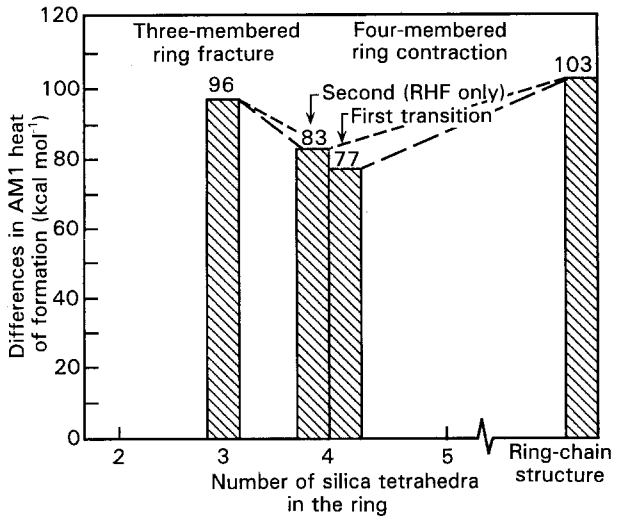

Figure 13 The differences in the AM1 barriers to water-free fracture for different sized silica structures.

ring. The transition state of four-fold ring fracture, shown in Fig. 9, has formed, or nearly formed, a trisiloxane ring which itself is not broken. Contraction to a three-fold ring, therefore, presents the crack tip with a much higher barrier to fracture. If there is another four-fold ring (or higher order ring) within the radius of the strain field at the crack tip, it will be redirected toward that structural feature rather than fracture a three-fold ring.

In the case of fracture of the Si–O bond in cyclotrisiloxane (a single D_2 ring), there are no smaller ring-like structures energetically possible in a transition state. The formation of a two-fold, disiloxane ring is very energetically unfavourable in vitreous silica, as discussed by Galeener [13] and Revesz and Gibbs [14]. Therefore, the fracture barrier for the three-fold ring of 96 kcal mol^{-1} is higher than the four-fold ring contraction which can proceed with a barrier of 77 kcal mol^{-1}.

5. Conclusion

The AM1 molecular orbital models indicate that a crack tip will move along lowest energy pathways. The crack will follow a path of four-fold D_1 (or larger) rings in vacuum or fast fracture. Fracture by water-free ring contraction has an energy barrier of 77 kcal mol^{-1} for four-fold rings. The fracture barrier for five-fold ring-chain structures is 103 kcal mol^{-1}. The barrier is 96 kcal mol^{-1} for fracture of a three-fold ring. The lower energy values for the larger structures is due to formation of transition states during fracture which produce trisiloxane-like rings. The transition states give rise to a quantitized ring contraction process, which is lower in energy but is still two to three times that of water-enhanced fracture, as seen in Part II. These findings predict that the fractal nature [5] of water free fracture will depend on the local concentration of cyclotetrasiloxane (four-fold ring) structures.

We hypothesize that the ring contraction mechanism occurs for all the ring structures (greater than three-fold) in vitreous silica during fracture. Fig. 14 presents a reaction scheme that directs the path of the

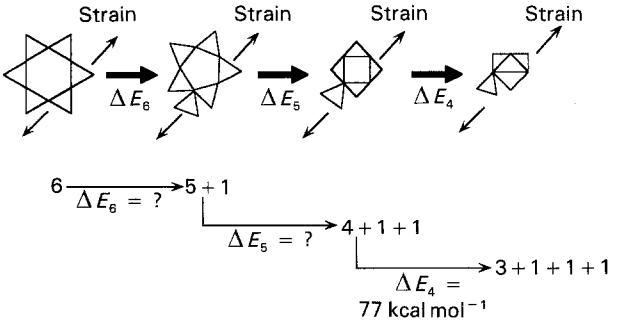

Figure 14 Ring concentration scheme for a-silica fracture.

crack tip during water-free fracture. The crack tip should follow a path of ring contraction as long as rings are near the crack tip. Ring contraction would be the preferred reaction path for fracture in a moisture-free environment. We expect that five- and six-membered rings will have an even lower barrier to ring contraction than the four-membered ring reported in this study. Part III in this series will address these details.

Acknowledgements

The authors gratefully acknowledge the support of the Air Force Office of Scientific Research, (Grant F49620-92-J-0351), and the Quantum Theory Project, UF. We also thank Larry Davis, Larry Burggraf and Mark Gordon for their technical support and encouragement. We also acknowledge the help and support of CaChe Scientific, Inc., Beaverton, OR.

References

1. C. E. INGLIS, *Trans. Inst. Nav. Arch.* **55** (1913) 219.
2. A. A. GRIFFITH, *Trans. R. Soc. Lond.* **221** (1921) 163.
3. S. W. FREIMAN, in "Glass Science and Technology", Vol. 5, "Elasticity and Strength in Glass", edited by D. R. Uhlmann and N. J. Kreidl (Academic Press, New York, 1980) pp. 21–79.
4. J. H. SIMMONS, T. P. SWILER and ROMULO OCHOA, *J. Non-Cryst. Solids* **134** (1991) 179.
5. J. J. MECHOLSKY Jr and S. W. FREIMAN, *J. Am. Ceram. Soc.* **74** (1991) 3136.
6. T. A. MICHALSKE and B. C. BUNKER, *J. Appl. Phys.* **56** (1984) 2686.
7. M. J. S. DEWAR, E. G. ZOEBISCH, E. F. HEALY and J. P. STEWART, *J. Am. Chem. Soc.* **107** (1985) 3902.
8. M. J. S. DEWAR and C. JIE, *J. Am. Chem. Soc.* **6** (1987) 1486.
9. MOPAC Version 6.1, Tektronix, Inc., CaChe Scientific, Beaverton, OR.
10. L. P. DAVIS and L. W. BURGGRAF, in "Ultrastructure Processing of Advanced Ceramics", edited by J. D. Mackenzie and D. R. Ulrich (Wiley, New York, 1988) p. 367.
11. L. W. BURGGRAF, L. P. DAVIS, and M. S. GORDON, in "Ultrastructure Processing of Advanced Materials", edited by D. R. Uhlmann and D. R. Ulrich (Wiley, New York, 1992) p. 47.
12. M. S. GORDON, Iowa State University (1993), private communication.
13. F. L. GALEENER, *J. Non-Cryst. Solids* **49** (1982) 53.
14. A. G. REVESZ and G. V. GIBBS, in "The Physics of MOS Insulators", edited by G. Lucousky, S. T. Pantelides and F. L. Galeener (Pergamon, New York, 1980) pp. 92–6.

Received 16 December 1993
and accepted 16 February 1994